Layer-1 Mobility in Distributed MIMO with Non-Coherent Joint Transmission

Peng Lin
Ericsson Research
Beijing, China
edwin.lin@ericsson.com

Omer Haliloglu
Ericsson Research
Istanbul, Turkey
omer.haliloglu@ericsson.com

***Abstract*—The Distributed Multiple Input Multiple Output (D-MIMO) network comprises a very large number of distributed Radio Units (RUs), which simultaneously serve multiple User Equipments (UEs) over the same time/frequency resources based on directly measured channel characteristics. Existing research had shown that Coherent Joint Transmission (CJT) in D-MIMO networks could obtain better performance compared to the traditional small cell and cellular massive MIMO network through multiple RUs. Nonetheless, reliable access links become more important at high frequency bands and mobility scenarios that needs robust precoding schemes to utilize the full performance of a D-MIMO network. In this paper, Physical layer (L1) mobility is incorporated in D-MIMO network operating at mmWave. Then centralized and distributed precoding methods are considered to evaluate the spectral efficiencies of mobile UEs with different serving RU subset update periodicities. Moreover, Non-Coherent Joint Transmission (NCJT) among multiple RUs is explored. Through the simulation results, it is shown that serving RU subset (cluster) update and NCJT substantially impact the performance. During UE mobility, frequent serving subset update is necessary for CJT, however, not critical for NCJT.**

***Index Terms*—Distributed MIMO, L1 mobility, channel aging, cluster update, coherent joint transmission, non-coherent joint transmission.**

I. Introduction

Both functional and deployment values will play a key role in 6G that should enable limitless connectivity. It will utilize higher frequencies and is supposed to give consumers greater high-speed data links and predictable Quality-of-Service (QoS), as well as being simple to deploy and adapt. Network densification and wideband transmission in high frequencies, as well as beamforming and efficient transport solutions considering multiple deployment options, will be critical for extreme performance. When small cell densification starts to suffer from interference, large-scale Distributed Multiple Input Multiple Output (D-MIMO), a.k.a. cell-free networks, can provide significant performance by coordinating distributed Radio Units (RUs) [1]. D-MIMO system can be thought of as a combination of Ultra Dense Networks (UDN) and Coordinated Multi-Point (CoMP) transmission [2], and in theory, there is no upper bound on capacity on D-MIMO with Coherent Joint Transmission (CJT), capacity can be increased by adding more RUs. It is only sort of impairments and practical limitations that will eventually be the limiting factor.

There is a further need to enable scalable D-MIMO considering practical approaches, e.g., non-coherent operation in higher bands. The ultimate solution would be CJT and centralized processing, however this will be difficult to implement. On the other hand, Non-Coherent Joint Transmission (NCJT) will result in spectrum inefficiency, but performance can be compensated with large bandwidth in higher frequency bands. Moreover, robust access links utilize macro diversity to overcome radio blocking that would need special attention in high frequency bands. Hence, the balance between complexity, robustness and performance need be investigated considering a broad range of frequency bands.

Recent studies have shown D-MIMO outperform traditional small cell and cellular massive MIMO networks in several practical scenarios [1]. The authors in [2] conducted a thorough investigation and introduced centralized/distributed transmit precoding and receive combining techniques. The authors in [3] developed a precoding technique that took into account overlapping clusters of RUs and centralized power control. In [4], the authors suggested distributed precoding techniques implemented by RUs with few antenna elements which provide interference cancellation. Various RU selection strategies are introduced in [5]–[8] motivated by practical implementation of D-MIMO systems. In [9], CJT in D-MIMO, which uses Spatial Repetition Transmission (SRT), has been investigated for centralized and interference-aware distributed precoding with User Equipment (UE) centric RU selection/clustering, and trade-off between implementation and deployment complexities has been shown. Authors in [10] formulated weighted sum rate maximization problem in non-coherent cell-free MIMO context and developed methods to solve user-scheduling and beamforming. Most of the studies regarding D-MIMO exclude time-varying propagation environment; however during mobility and high carrier frequency operation channel aging effect becomes visible [11]. The impact of channel aging has been studied in collocated massive MIMO systems [12], [13], and authors in [14] first investigate the impact of channel aging in the D-MIMO context with pilot contamination. In [15], the impact of channel aging was investigated on the performance of precoding in D-MIMO considering UE mobility and phase noise. To the best of our knowledge, this study is the first study that analyzes the impact of serving cluster update and its periodicity for downlink (DL) precoding in D-MIMO network including channel aging effect due to UE mobility. Moreover, performance of NCJT has

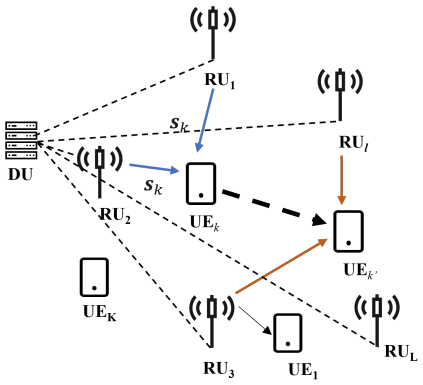

Fig. 1. L1 mobility in D-MIMO with spatial repetition transmission.

also been evaluated for distributed and centralized precoding schemes with channel aging.

This work presents the following contributions:

- Centralized/distributed precoding are studied with physical Layer (L1) mobility, i.e., serving RU subset update.
- NCJT using SRT among multiple RUs is explored in a D-MIMO setup.
- The impact of serving subset and precoder update periodicities are examined for both CJT and NCJT.

II. SYSTEM MODEL

A D-MIMO network consisting of L RUs and K UEs is shown in Fig. 1, where all RUs are connected to the Distributed Unit (DU) through high-capacity fronthaul links (e.g., fiber-optic cables). The geographically distributed RUs can serve all UEs in the same time-frequency resource block. It is assumed that each RU and UE are equipped with single antenna, but it is straightforward to extend to the multi-antenna case. All RUs can be well-planned or randomly located throughout the area and are assumed to have perfect channel information. Let $s_k, k = 1, 2, \ldots, K$, denotes the information data intended the k-th UE, where $\mathbb{E}\{s_k s_j^*\} = 1$ for $j = k$, zero otherwise, where $\mathbb{E}\{\cdot\}$ is the expectation operator. Then, the transmitted data from the l-th RU to K UEs can be expressed as $x_l = \sum_{k=1}^{K} w_{l,k} s_k$ where $w_{l,k} \in \mathbb{C}^{1\times 1}$ is the precoding weight at the l-th RU for the transmission intended for the k-th UE.

A. L1 Mobility

In addition to coordinated densification and macro-diversity overcoming the path-loss and removing the blocking effect for uniform performance, D-MIMO also helps realizing robust access links that supports L1 mobility on high frequency bands where the propagation environment is more challenging. Following a UE-centric approach, dynamic RU-UE association algorithms update the serving RU subset for each UE, reducing the amount of unwanted higher layer handovers that creates time-consuming signaling [5]. RUs are grouped in a UE-centric way to serve the UEs, typically the ones that provide a sufficiently high Signal-to-Noise-Ratio (SNR). The serving subsets for neighboring UEs are partially overlapping, thus the RUs cannot always be divided into disjoint sets, as in traditional cellular networks. The precoder must be updated when serving RU subset has been updated. The RU subsets, on the other hand, may not require as frequent updates as the precoder because the key factor for RU-UE association is slow fading which is mainly affected by the distance to the RUs.

In the scenario depicted in Fig. 1, where multiple RUs (RU_1 and RU_2) simultaneously serve k-th UE. When the UE moves to a new position, serving RU subset will be updated based on the large scale fading coefficients. Thus, the UE will continuously achieve sufficiently high SNR via updated serving RU subset. The serving RU subset selection and updates can be performed centrally at the DU which has the channel information for all UE. Each RU can simultaneously serve a limited number of UEs, where RUs prioritize the UEs with better channel qualities.

B. Data Transmission

Channel reciprocity within Time Division Duplex (TDD) is assumed such that Uplink (UL) channel estimates are used in DL transmission. Given that L RUs serve K UEs, $\mathbf{H} \in \mathbb{C}^{K\times L}$ denotes the complex channel matrix and the channel coefficient between the l-th RU and k-th UE is modeled as

$$h_{k,l} = g_{k,l} \cos\left(\varphi_{k,l} t + \theta_{k,l}\right) \tag{1}$$

where $g_{k,l}$ is the channel gain between the l-th RU to k-th UE. $\theta_{k,l} \sim \text{U}(-\pi,\pi)$ denotes initial phase, which follows uniform random distribution from $-\pi$ to ,π. $\varphi_{k,l}$ is the angular frequency which is obtained as $\varphi_{k,l} = 2\pi(\frac{f}{c} v_k \cos(\alpha_{k,l}))$ where c denotes the speed of light, f is the carrier frequency, v_k is the velocity of k-th UE, and $\alpha_{k,l}$ is the angle between k-th UE's moving direction and l-th RU. Given that each RU has the same transmission power limit denoted by P, the received signal for the k-th UE can be expressed as

$$y_k = \sum_{l=1}^{L_k} \sqrt{P} h_{k,l} w_{l,k} s_k + \sum_{j=1, j\neq k}^{K} \sum_{l=1}^{L_j} \sqrt{P} h_{j,l} w_{l,j} s_j + n_k, \quad \forall k \tag{2}$$

where the first term denotes intended signal received from the serving RU set of size L_k for the k-th UE, second term is the interference, and n_k represents the zero mean circularly symmetric additive white Gaussian noise with variance σ_k^2.

Phase CJT: Intended signal strength can be maximized at the receiver, by adding the signals from multiple RUs phase coherently such that phase of the precoding coefficient is chosen to match the phase of channel between the RU and intended UE, i.e., $\angle w_{lk} \triangleq -\angle h_{kl}$ for all l, k.

Phase NCJT: Precoding coefficients, $w_{l,k}$, are calculated by using only large scale fading, and signals from multiple RUs are added phase non-coherently at the receiver

Received signal vector for K UEs, $\mathbf{y} \in \mathbb{C}^{K\times 1}$, is written as

$$\mathbf{y} = \sqrt{P}\mathbf{H}\mathbf{W}\mathbf{s} + \mathbf{n} \tag{3}$$

where $\mathbf{W} \in \mathbb{C}^{L\times K}$ is the precoding matrix that can be calculated centrally in DU or in a distributed way in each RU, $\mathbf{s}$ is transmitted information bearing signal vector to K UEs, and $\mathbf{n}$

is the noise vector. Based on Eq. (3), the signal-to-interference-plus-noise-ratio (SINR, γ) of k-th UE can be calculated as

$$\gamma_k = \frac{P\Big[(\mathbf{HW})^{\mathrm{H}}(\mathbf{HW})\Big]_{k,k}}{\sigma_k^2 + P\sum\limits_{j=1, j\neq k}\Big[(\mathbf{HW})^{\mathrm{H}}(\mathbf{HW})\Big]_{k,j}} \tag{4}$$

where $(\cdot)^{\mathrm{H}}$ is the Hermitian transpose operator, $[.]_{k,j}$ denotes (k,j)-th entry of the matrix. Then, average DL Spectral Efficiency (SE) per UE can be obtained as

$$r = \frac{1}{K}\sum_{k=1}^{K}\log_2(1+\gamma_k) \tag{5}$$

C. Precoding with Channel Aging

Accurate channel estimation becomes crucial during mobility and high frequency operation that incorporates channel aging effects due to the time-varying propagation environment, i.e., the channel varies between when it is estimated at the RU and when it is used for processing [7]. Given the channel reciprocity, the received signal in Eq. (3) is expressed as

$$\mathbf{y} = \sqrt{P}\mathbf{H}\tilde{\mathbf{W}}\mathbf{s} + \mathbf{n} = \sqrt{P}(\mathbf{G}+\tilde{\mathbf{G}})\tilde{\mathbf{W}}\mathbf{s} + \mathbf{n} \tag{6}$$

where $\mathbf{G} \in \mathbb{C}^{K\times L}$ denotes the estimated channel matrix and $\tilde{\mathbf{G}} \in \mathbb{C}^{K\times L}$ is the bias matrix incorporating the channel aging impact. $\tilde{\mathbf{W}} \in \mathbb{C}^{L\times K}$ denotes the precoding matrix calculated by using estimated channel matrix $\mathbf{G}$, such that $\mathbf{G}\widetilde{\mathbf{W}} = \mathbf{I}$, where $\mathbf{I}$ is the identity matrix; however, the received signal quality at the UEs will still face the effect of the bias matrix $\tilde{\mathbf{G}}$. To be specific, assuming that all RUs forming a single serving subset to all UEs with $L \geq K$, a centralized precoding scheme based on zero forcing [8] can be formulated as

$$\tilde{\mathbf{W}} = \mathbf{G}^{\mathrm{H}}(\mathbf{G}\mathbf{G}^{\mathrm{H}})^{-1}. \tag{7}$$

Additionally, a subset of RUs can create a UE specific cluster that is, these RUs serve UEs inside the given cluster where the channel matrix is denoted by $\mathbf{G}_k$, but also creates interference to the UEs outside of the cluster where the interference channel matrix is represented by $\mathbf{F}_k$. Interference Aware Distributed Zero Forcing (IADZF) were analyzed and compared with Centralized Zero Forcing (CZF) in [9]. UE-centric precoders per each subset can be expressed as

$$\tilde{\mathbf{W}}_{\mathbf{k}} = \mathbf{G}_k^{\mathrm{H}}(\mathbf{G}_k\mathbf{G}_k^{\mathrm{H}} + \mathbf{\Lambda}_{\mathbf{k}})^{-\mathbf{1}}, \tag{8}$$

where $\mathbf{\Lambda}_k = \mathbf{F}_k\mathbf{F}_k^H$ denotes the interference covariance matrix for k-th serving subset, then each UE-centric precoder will be combined as given in [9] to achieve $\tilde{\mathbf{W}}$. Eq. (8) considers the case of $L_k \geq K-1$, i.e., number of transmit antennas in the serving subset is still more than the number of receive antennas outside of the cluster to whom the precoder tries to minimize the interference; however in other cases, precoder might need to consider left inverse based on the rank of $\mathbf{G}_k$. Eventually, the received signal vector will be obtained as

$$\mathbf{y} = \sqrt{P}\mathbf{s} + \mathbf{n} + \sqrt{P}\tilde{\mathbf{G}}\tilde{\mathbf{W}}\mathbf{s}, \tag{9}$$

where the last term exists due to channel aging is scaled by precoder that will eventually degrade the performance.

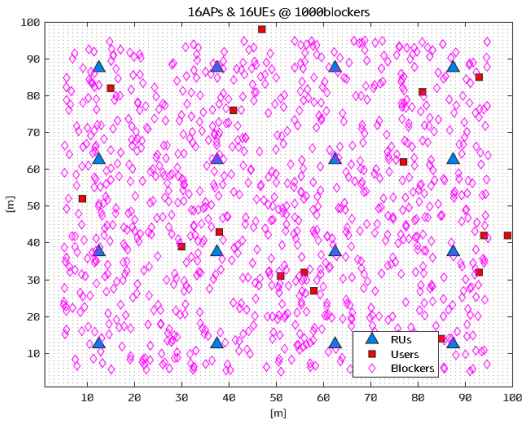

Fig. 2. Deployment scenario with 16 RUs, 16 UEs, and 1000 blockers.

III. PERFORMANCE EVALUATION

In this section, the performance of the D-MIMO system with L1 mobility and NCJT operating at 28 GHz is analyzed in a DL indoor scenario. The scenario is given in Fig. 2 within the area of 100m × 100m with randomly distributed 1000 blockers with maximum size of 2m × 3m and minimum size of 0.5m × 1m. Different number of RUs are regularly deployed and $K = 16$ UEs are randomly dropped in the area. During L1 mobility, different periodicities are considered to update the serving RU subset. Other simulation parameters are given in Table I. Perfect channel estimation and fronthaul is assumed.

When phase information is available for the precoding calculation in DU, the SE performance with different number of serving RUs with 100ms update periodicity is shown in Fig. 3. It has been shown that if total number of deployed RUs increases, SE will be improved for both centralized and UE-centric distributed precoding methods since interference can be better mitigated by increased degrees of freedom within the available candidate RUs. When the UE is mobile and associates with one RU which is updated at each 100ms, distributed and centralized precoding will perform similarly. As serving subset enlarges, i.e., number of serving RUs increases, the performance difference between two precoding schemes also scales up. For the centralized precoding, when serving subsets having 2 or 4 RUs, SE will be improved obviously. But for the distributed precoding, when serving RU subset enlarges within a deployment of less candidate RUs, the performance

TABLE I
SIMULATION MODEL SPECIFICATIONS

Parameters	Model specifications
Operating frequency (GHz)	28
Bandwidth (MHz)	200
RU max power (dBm)	13
Propagation Model	3GPP InH [16]
Duplexing	TDD with 50% DL
Channel coherence time (ms)	100
Serving RU subset update periodicity (ms)	100, 500
UE speed (m/s)	5

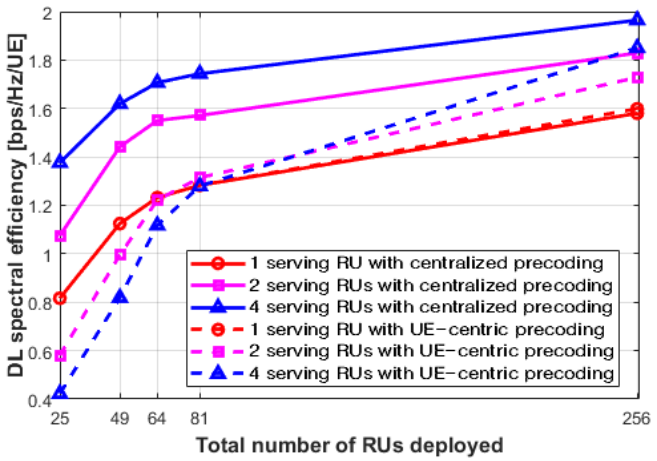

Fig. 3. SE performance of centralized and distributed precoding with CJT for different number of serving RUs in a scenario with 16 UEs.

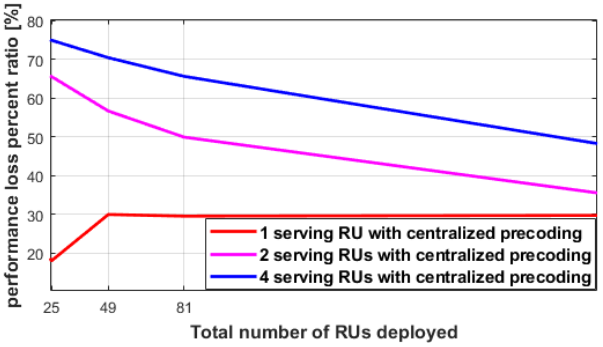

(a) Centralized precoding.

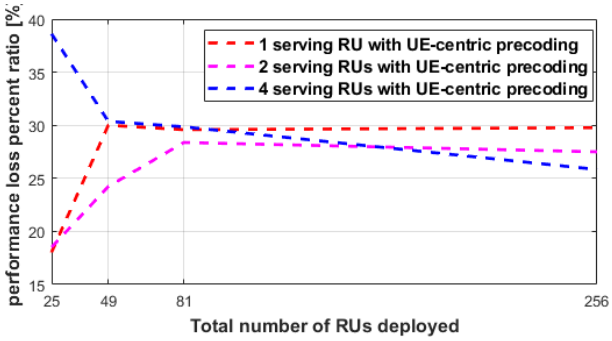

(b) Interference aware distributed precoding.

Fig. 4. Performance loss ratio for centralized precoding and distributed precoding when serving RU subset update periodicity is 500ms.

decreases since more interference starts to exist in the UE-specific clusters. However, in case of dense RU deployment, larger serving subsets can attain better performance.

In order to observe the SE performance loss due to the longer serving subset update periodicity, e.g., 500 ms, a metric of performance loss ratio is defined as $\eta = \frac{SE_{100ms} - SE_{500ms}}{SE_{100ms}} \times 100\%$ With a serving subset update periodicity of 500ms, the performance loss ratios, η, for centralized precoding and interference aware distributed precoding are shown in the Fig. 4. It

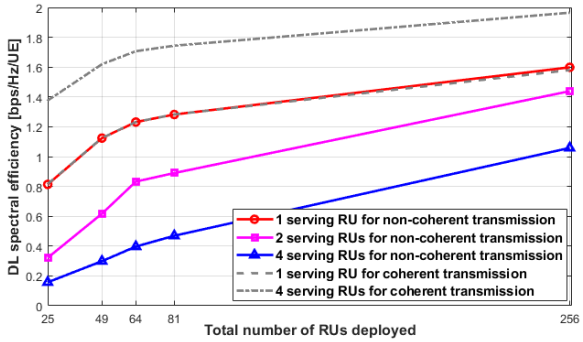

(a) centralized precoding.

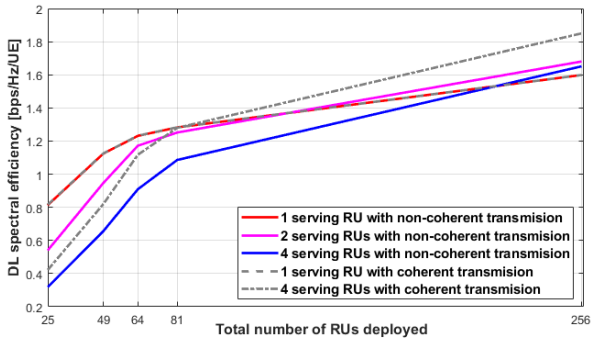

(b) Interference aware distributed precoding.

Fig. 5. SE performance of for phase CJT and NCJT schemes for different number of serving RUs in the scenario with 16 UEs when serving RU subset update periodicity is 100ms.

is shown that when longer RU update periodicity is adopted, the performance of both precoding schemes will be degraded. Specifically, when a mobile UE has associated to one RU under the long update periodicity, performance loss increases by the increasing number of total RUs due to the increased performance for frequent update. However, the performance variation will be different in case of multiple serving RUs in which for centralized precoding, the performance loss is more obvious in small number of total deployed RUs, however, better performance can be obtained with more available RUs. For distributed precoding, in case of a subset of 4 RUs, the decreasing loss behavior is similar to centralized precoding but with less performance loss. Additionally, one should note that centralized precoding outperforms distributed scheme for 100 ms update, but loses more performance with slower updates.

When channel phase information is not known in precoding operation, the SE performance per UE is shown in Fig. 5. To observe the impact of phase NCJT, it is compared with CJT for different number of serving RUs. NCJT attains less performance in multiple serving RU subsets relative to the CJT due to the not-optimized parameters. Since distributed precoding considers sub-group performance optimization, which already decreases performance, NCJT will cause relatively less performance loss compared with centralized precoding.

As shown in Fig. 4 and Fig. 5, centralized and distributed

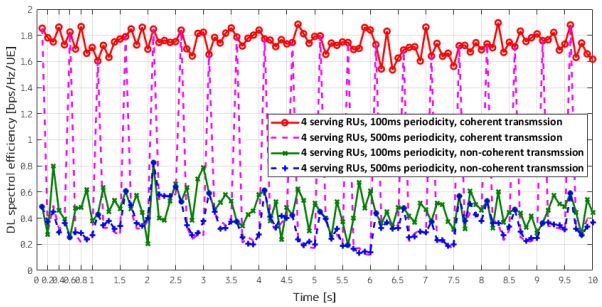

(a) centralized precoding.

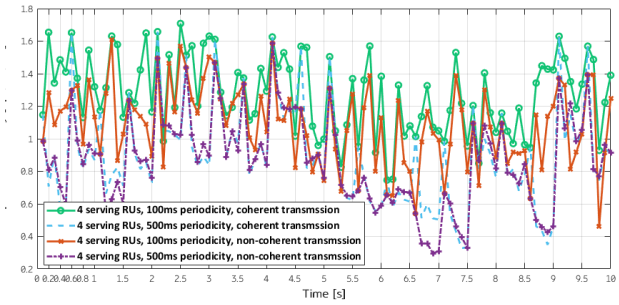

(b) Interference aware distributed precoding.

Fig. 6. SE behavior evaluated in 10s time frame, for CJT and NCJT schemes with serving subset size of 4 RUs and different subset update periodicities.

precoding schemes perform differently for longer serving RU subset update periodicities and NCJT. To clearly reflect these effects, performance variation is evaluated for both precoding schemes with 4 serving RUs out of 81 deployed RUs within 10 seconds. Fig. 6 illustrates the performance of precoding schemes when longer periodicity and NCJT are adopted for mobile UEs. For centralized precoding as shown in Fig. 6 (a), when long periodicity is adopted, SE fluctuates with serious degradation since not frequently optimized precoder is used between successive updates. Moreover, when phase coherency is excluded, regardless of 100ms or 500ms update periodicity, the performance is substantially reduced, and performance is similar with CJT under long update periodicity. For distributed precoding, performance fluctuation is observed for both update periodicities, nonetheless, the varying performance in centralized precoding for different update periodicities is disappeared. Additionally, for NCJT, although SE will be reduced, the impact of update periodicity is smaller than that for CJT.

IV. CONCLUSIONS

In this paper, L1 mobility scheme is investigated in D-MIMO system with centralized and interference aware distributed precoding methods for both phase CJT and NCJT schemes to evaluate its performance and robustness under different serving RU subset update periodicities. Through the simulation results, it is shown that when the UE is mobile, and short serving RU update periodicity and CJT are adopted for DL transmission, the centralized precoding has better performance compared with respect to interference-aware distributed precoding method. However, when longer serving RU subset update periodicities and NCJT are considered, the performance will be degraded. Despite its low performance of distributed precoding, it can still provide robust performance with respect to longer RU update periodicity and NCJT. Moreover, during UE mobility, frequent serving subset update is necessary for CJT, however, it is not critical for NCJT.

ACKNOWLEDGMENT

This work was supported by The Scientific and Technological Research Council of Turkey (TUBITAK) through the 1515 Frontier Research and Development Laboratories Support Program under Project 5169902, and has been partly funded by the European Commission through the H2020 project Hexa-X (Grant Agreement no. 101015956).

REFERENCES

[1] H. Q. Ngo, A. Ashikhmin, H. Yang, E. G. Larsson, and T. L. Marzetta, "Cell-free massive MIMO versus small cells," *IEEE Transactions on Wireless Communications*, vol. 16, no. 3, pp. 1834–1850, 2017.

[2] S. Chen, J. Zhang, J. Zhang, E. Björnson, and B. Ai, "A survey on user-centric cell-free massive MIMO systems," *arXiv preprint arXiv:2104.13667*, 2021.

[3] A. Ö. Kaya and H. Viswanathan, "Dense distributed massive MIMO: Precoding and power control," in *IEEE INFOCOM 2020-IEEE Conference on Computer Communications*. IEEE, 2020, pp. 756–763.

[4] G. Interdonato, M. Karlsson, E. Björnson, and E. G. Larsson, "Local partial zero-forcing precoding for cell-free massive MIMO," *IEEE Transactions on Wireless Communications*, vol. 19, no. 7, pp. 4758–4774, 2020.

[5] S. Buzzi and C. D'Andrea, "Cell-free massive MIMO: User-centric approach," *IEEE Wireless Communications Letters*, vol. 6, no. 6, pp. 706–709, 2017.

[6] H. Q. Ngo, H. Tataria, M. Matthaiou, S. Jin, and E. G. Larsson, "On the performance of cell-free massive MIMO in ricean fading," in *2018 52nd Asilomar Conference on Signals, Systems, and Computers*. IEEE, 2018, pp. 980–984.

[7] S. Chen, J. Zhang, E. Björnson, J. Zhang, and B. Ai, "Structured massive access for scalable cell-free massive MIMO systems," *IEEE Journal on Selected Areas in Communications*, 2020.

[8] C. D'Andrea and E. G. Larsson, "User association in scalable cell-free massive MIMO systems," in *2020 54th Asilomar Conference on Signals, Systems, and Computers*. IEEE, 2020, pp. 826–830.

[9] O. Haliloglu, J. Sadreddini, and P. Frenger, "Interference-aware distributed precoding in coherent large-scale distributed MIMO," in *2021 IEEE Globecom Workshops (GC Wkshps)*. IEEE, 2021, pp. 1–6.

[10] H. A. Ammar, R. Adve, S. Shahbazpanahi, G. Boudreau, and K. Srinivas, "Resource allocation and scheduling in non-coherent user-centric cell-free MIMO," in *ICC 2021-IEEE International Conference on Communications*. IEEE, 2021, pp. 1–6.

[11] K. T. Truong and R. W. Heath, "Effects of channel aging in massive MIMO systems," *Journal of Communications and Networks*, vol. 15, no. 4, pp. 338–351, 2013.

[12] A. K. Papazafeiropoulos, "Impact of general channel aging conditions on the downlink performance of massive MIMO," *IEEE Transactions on Vehicular Technology*, vol. 66, no. 2, pp. 1428–1442, 2016.

[13] R. Chopra, C. R. Murthy, H. A. Suraweera, and E. G. Larsson, "Performance analysis of FDD massive MIMO systems under channel aging," *IEEE Transactions on Wireless Communications*, vol. 17, no. 2, pp. 1094–1108, 2017.

[14] J. Zheng, J. Zhang, E. Björnson, and B. Ai, "Cell-free massive MIMO with channel aging and pilot contamination," in *GLOBECOM 2020-2020 IEEE Global Communications Conference*. IEEE, 2020, pp. 1–6.

[15] W. Jiang and H. D. Schotten, "Impact of channel aging on zero-forcing precoding in cell-free massive MIMO systems," *IEEE Communications Letters*, vol. 25, no. 9, pp. 3114–3118, 2021.

[16] J. Meredith, "Study on channel model for frequency spectrum above 6 GHz," *3GPP TR 38.900, Jun, Tech. Rep.*, 2016.